Surface & Coatings Technology 439 (2022) 128447

Contents lists available at ScienceDirect

Surface & Coatings Technology

journal homepage: www.elsevier.com/locate/surfcoat

Surface finishing and residual stress improvement of chemical vapour deposited tungsten carbide hard coatings by vibratory polishing

Christian Micallef [a,b], Karl Walton [c], Yuri Zhuk [b], Adrianus Indrat Aria [a,*]

[a] Surface Engineering and Precision Centre, School of Aerospace, Transport and Manufacturing, Cranfield University, MK43 0AL, United Kingdom
[b] Hardide Coatings Plc, Bicester OX26 5AH, United Kingdom
[c] University of Huddersfield, Department of Engineering and Technology, School of Computing and Engineering, HD1 3DH, United Kingdom

ARTICLE INFO

Keywords:
Vibratory polishing
Tungsten carbide
Surface roughness
Residual stress

ABSTRACT

Hard coatings are widely used in several industries to improve the service life of engineering components. W/WC coatings deposited through chemical vapour deposition (CVD) have the capability of providing the required protection on parts with complex geometries, commonly used in high wear and corrosive environments. Despite the improvement in service life, a key important factor is the adherence to low roughness and tolerance specifications, necessitating the need of a post-coating finishing process. In this work the impact of vibratory polishing on W/WC coating was studied using a vibratory barrel setup and two types of ceramic-based media. An improvement in average Ra of 0.2–0.3 μm was achieved over a duration of 4 h with abrasive wear being the predominant polishing mechanism. Insignificant weight loss (<0.017 g) and hardness changes ($-2 < \Delta HV < 8$) were confirmed while the compressive residual stresses of the coating were found to increase with process time (max $\Delta\sigma = -1058.3$ MPa).

1. Introduction

Modern engineering components, such as turbine blades, engine piston pumps and flow control valves, often operate in extremely harsh conditions throughout their operating lifetime [1–3]. For example, flow control components used in the petrochemical industry are subjected to high repetitive loads and corrosive conditions [4,5]. Protective hard coatings are typically applied on the surface of these components to prolong their service life and to minimise the likelihood of catastrophic failure. The application of hard coatings is therefore of benefit to many applications as an effective and cost-efficient means of improving their wear and corrosion resistance. Existing hard coatings, including the widely used cemented carbide, transition-metal carbides and nitrides and diamond-like carbon (DLC), exhibit hardness values exceeding 1000 HV and wear rates in the order of 10^{-6}–10^{-8} mm^3/Nm range [6–8]. A novel tungsten carbide in tungsten matrix (W/WC) coating is one of the most promising hard coatings due to their superlative hardness and wear rate [4,9–12]. In addition, W/WC coating can be deposited through chemical vapour deposition (CVD) technique to eliminate the use hexavalent precursors which are restricted by the Registration, Evaluation, Authorisation and Restriction of Chemicals (REACH) regulation [13]. CVD itself is a versatile non-line-of-sight technique capable of depositing advanced materials on parts with complex geometries [11,14–16]. Our previous investigations have shown that CVD W/WC coating has a matt grey texture with relatively high surface roughness in the as-deposited condition that requires a surface finishing action to improve its surface texture, particularly in the difficult to access areas with complex geometries [10]. A surface finishing process capable of reaching W/WC coating in these difficult to access areas is therefore required.

Amongst many available surface finishing techniques, vibratory polishing has the potential to address this issue through its presumed capability to process parts with complex geometries. Vibratory polishing is a mass finishing technique commonly used for deburring, edge radiusing, surface finishing, surface smoothing, and cleaning. While this topic is worth more consideration and comprehensive scrutiny, research into vibratory polishing revolves predominantly around uncoated metallic materials, such as stainless steels, titanium, and aluminum [17–22]. The use of vibratory polishing on engineering components with hard coatings is thus far very limited to cemented carbide coatings. Previous study has shown that vibratory polishing of cemented carbide containing 15–20 wt% of soft Co binder leads to a significant loss of soft binder due to a difference in hardness and ductility of the different phases [23]. In contrast, the CVD W/WC coatings studied herein are not

* Corresponding author.
E-mail addresses: C.Micallef@cranfield.ac.uk (C. Micallef), k.walton@hud.ac.uk (K. Walton), yzhuk@hardide.com (Y. Zhuk), A.I.Aria@cranfield.ac.uk (A.I. Aria).

https://doi.org/10.1016/j.surfcoat.2022.128447
Received 9 March 2022; Received in revised form 5 April 2022; Accepted 10 April 2022
Available online 21 April 2022

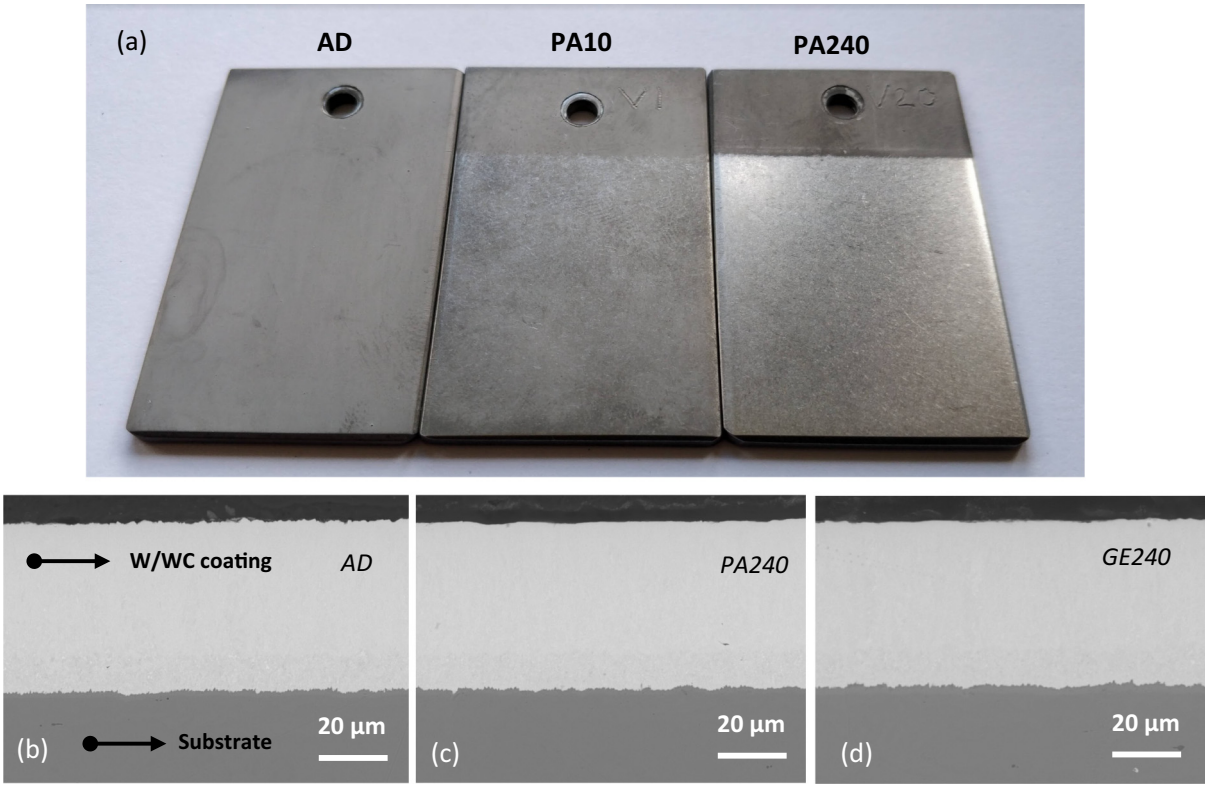

Fig. 1. (a) Photograph of W/WC coated samples in the AD, PA10 and PA240 conditions, cross-sectional SEM images of (b) AD prior to (c) PA240 testing and (d) GE240 testing.

expected to suffer from such selective material removal behaviour due to their binderless nature. As reported in our previous studies, our CVD W/WC coatings are structurally homogenous and pore-free [10,11,24].

In this work we systematically report the impact of vibratory polishing on hard CVD W/WC coatings with respect to coating morphology, surface roughness, and residual stresses. We found that vibratory polishing is an effective surface finishing technique causing negligible material loss and preferential material removal. Our findings demonstrate the potential capability of vibratory polishing in providing sufficient surface finishing quality without sacrificing the integrity of the W/WC coatings. Our approach and analysis establish a basis for further study into vibratory polishing to enable surface finishing of hard coatings that will be of relevance to numerous engineering applications.

2. Experimental procedure

A set of 25 × 50 mm rectangular coupons were cut from commercial-grade 304 stainless steel sheet with a thickness of 3 mm. Tungsten/tungsten carbide (W/WC) coating was deposited on the samples by Hardide Coatings Ltd. (Bicester, Oxford-UK) at a temperature of 500 °C. The deposited coating is composed of tungsten carbide nano-particles dispersed in a tungsten metal matrix and is crystallised atom-by-atom from a gas mixture, producing a conformal coating with a negligible porosity of <0.05% (Fig. SI 1) [10,11,24]. The as-deposited coatings, denoted herein as AD, have an average microhardness of 1330 ± 41 $HV_{0.1}$ (Zwick ZHVμ, Vickers) and nominal coating thickness of 50–55 μm.

A desktop vibratory polisher (PDJ Vibro, SB Range) with a gross volume of 7 l and a height of 495 mm was used in this work (Fig. SI 2). The polisher consists of a heavy-duty polymer bowl, a chute used for unloading the abrasive media and the processed parts, a sound cover, and a heavy-duty stand made up of moulded polyethylene with rubber pads on the bottom. The vibratory motion in the rig is generated via an electric motor, which is attached to the bottom of the vibratory bowl, with a power of 0.18 kW (0.25 hp). Two types of Alumina-based abrasive media with a Vickers hardness greater than 2300 HV were used in this work. They included pink aggi (PA) with a tristar geometry and grey ellipse (GE) with an elliptical geometry (Fig. SI 3a-b). The rationale for selecting these two media, without prior knowledge of the impact of the media on hard materials, was primarily based on the superior hardness of the ceramic media which are commercially available. As PA media are typically used for producing finer finisher, this was selected to assess whether a finer finish would be produced in comparison to GE. Samples were tested at incrementally increased time durations starting at 10 min up to 240 min. Here, the coated samples after being subjected to vibratory polishing are denoted by the type of media and polishing time. For example, PA10 and PA240 correspond to samples that have been polished for 10- and 240-min using pink aggi media. Similarly, GE annotation refers to samples tested with grey-ellipse media. For example, GE240 corresponds to the sample tested for 240-min using grey ellipse media.

Scanning electron microscope (SEM, Tescan Vega) was used to characterise the surface morphology. Atomic force microscopy (AFM, Digital Instruments) with a silicon scanning probe and a scan surface area of 60 × 60 μm^2 was used to map the surface topography of the samples and monitor the changes over time. A 3D non-contact surface profiler (Taylor Hobson) with a 20× objective and a sampling scale of 900 × 900 μm was used to characterise the surface roughness of the samples. The data sets were filtered with a Gaussian filter with an L filter nesting index of 0.8 mm. In this work, an X-Ray diffractometer (Siemens D5005) using $Cu - K\alpha$ radiation ($\lambda = 0.15405$ nm) was used to perform X-Ray diffraction on the samples. A 2θ range of 30° to 140° was used at a scanning step time of 0.02°/s using a tube acceleration voltage of 40 kV and a current of 40 mA. The $sin^2\psi$ method was employed to measure the magnitude and nature of the residual stresses in the coatings. The residual stress of each tested samples was initially measured in the as-

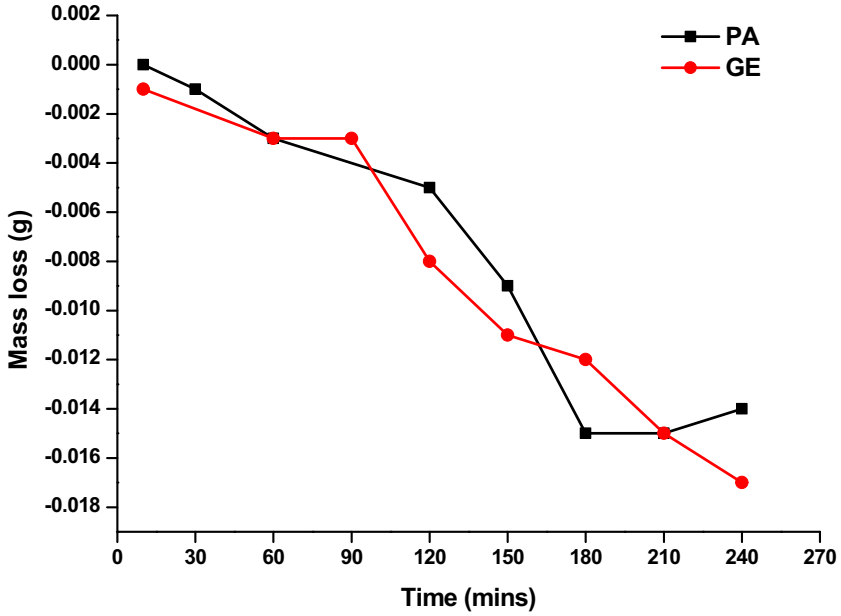

Fig. 2. Mass loss as a function of process time using PA and GE media.

deposited condition and subsequently in the vibratory polished condition. This enabled the determination of any changes in the residuals stresses as a consequence of the vibratory polishing process. For residual stress measurements, nine ψ angles in the -45° to 45° range were used at a step size of 0.01° per second while the $W\{310\}$ peak at $2\theta = 96^\circ$ to 104° was used. This peak was purposefully selected at a high angle to be able to have measurable changes in the 2θ as otherwise, at small angles, the incremental peak shift would be too small to be measured [25].

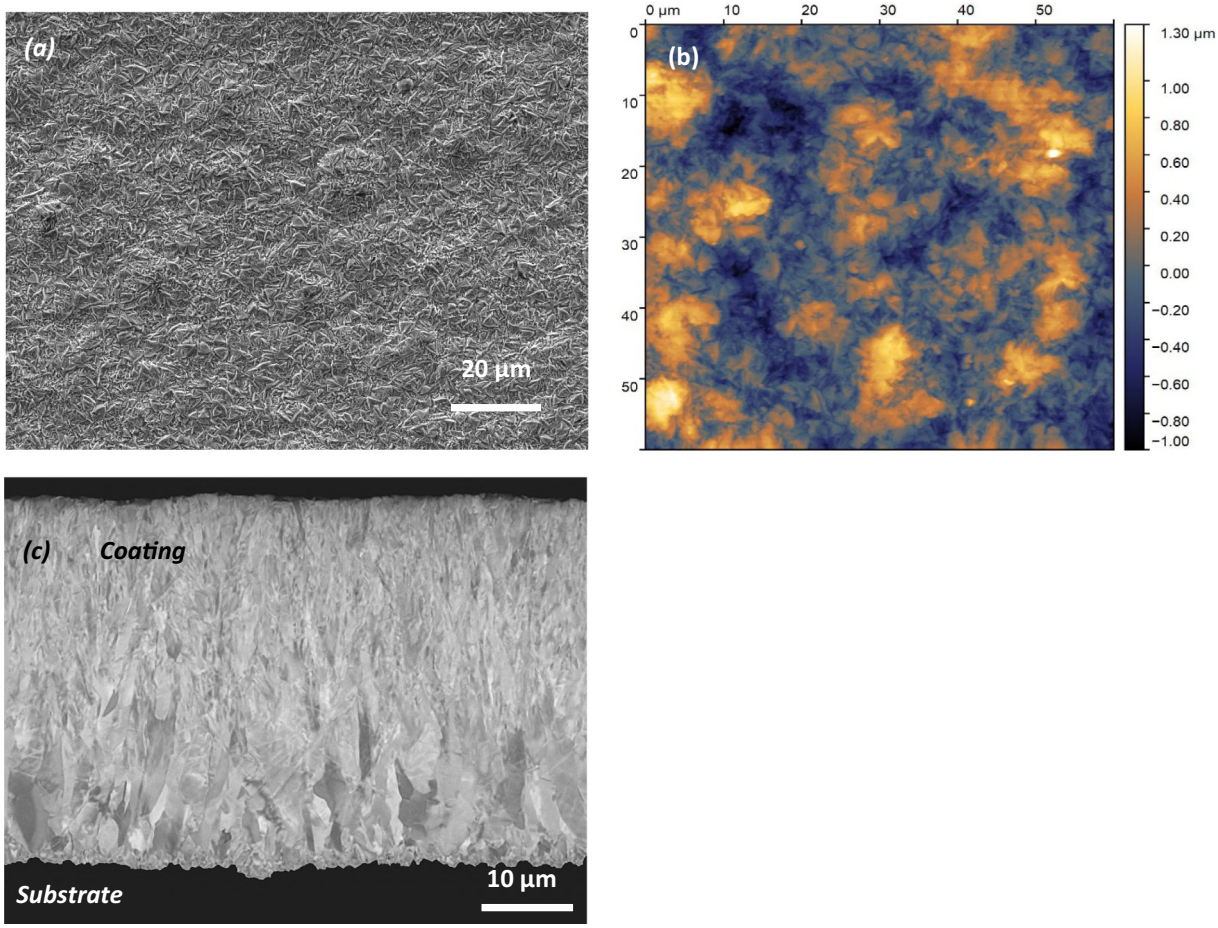

Fig. 3. (a) SEM and (b) AFM surface view of as-deposited coating and (c) cross-sectional view of etched W/WC coating showing a columnar coating structure.

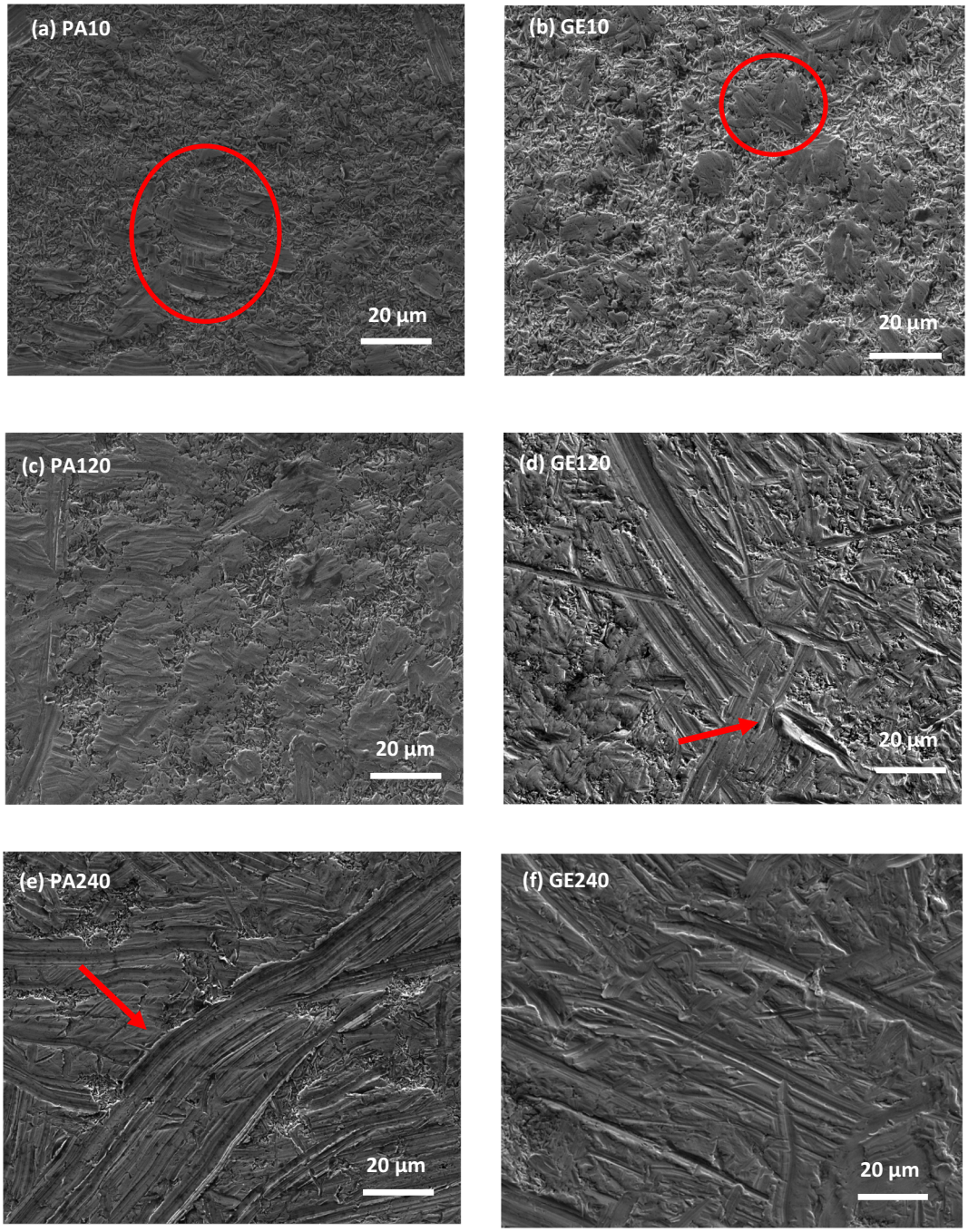

Fig. 4. Top view SEM images showing surface morphologies of (a) PA10 showing initial light scratching due to rolling contact (b) GE10 showing localised flattening, (c) PA120, (d) GE 120 showing the formation of surface indentations, (e) PA240 showing the effects of micro-ploughing and (f) GE240.

Other considerations in selecting this peak were that no other peaks were present in its close proximity so as to avoid any interference or possible overlapping. It was also essential that the peak would be differentiated from any background noise. The residual stresses were calculated using (Eq. (1)) through the DIFFRAC.PLUS software by Bruker.

$$\sigma_{\varnothing} = \left(\frac{E}{1+\nu}\right)m \tag{1}$$

3. Results

The change in surface texture of W/WC coatings after being subjected to vibratory polishing can be seen visually (Fig. 1a), where the matte surface texture of the as-deposited coating becomes glossier with the increase in polishing time. A change in the coating surface texture could be observed within just 10 min of vibratory motion, which continued to become increasingly significant as the process time increased. At a maximum polishing duration of 240 mins, the W/WC coating exhibited a relatively glossy surface texture across the entire surface of the coating. The glossy surface texture suggests a significant reduction in surface roughness. This is confirmed by cross-sectional SEM images, where those of PA240 and GE240 showed that much smoother coating surfaces when compared to the as-deposited surfaces (Fig. 1b-d). Note that a negligible change in coating thickness (Fig. 1b-d) and mass were recorded (Fig. 2). A coating thickness of 48 ± 4 µm is observed on

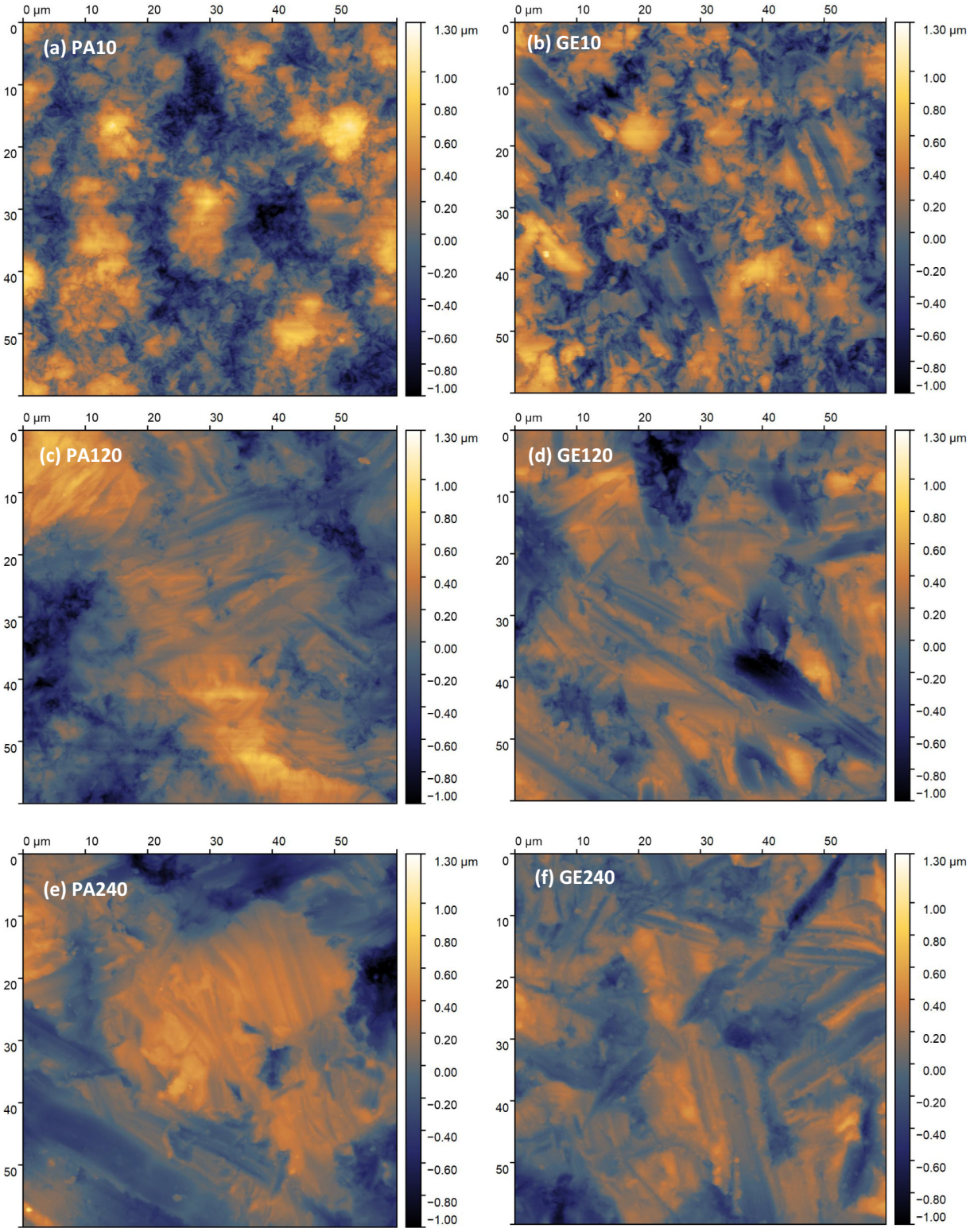

Fig. 5. AFM surface profiles of (a) PA10, (b) GE10, (c) PA120, (d) GE 120, (e) PA240 and (f) GE240.

all samples, including AD, PA240, and GE240 samples.

The changes in surface topography of the coating as a function of polishing time using PA and GE media is analysed qualitatively and quantitatively using SEM and AFM, respectively. The surface of AD samples exhibits a grainy appearance with approximate grain sizes of 1–3 µm and an average arithmetic roughness (Ra) of 0.4 ± 0.03 µm (Fig. 3a-b). Such a grainy surface morphology can be attributed to the columnar growth of W/WC coatings, where the surface is made up of numerous distinctive columnar grains and grain orientations (Fig. 3c). Note that columnar microstructure is often observed on crystalline coatings grown by CVD which is established by the flow of the precursor gases and their mass transport [3,11,26]. The surface of samples PA10 and GE10 subjected to 10 min of vibratory polishing exhibit patchy micro-wear tracks formed by the rolling action of the abrasive media

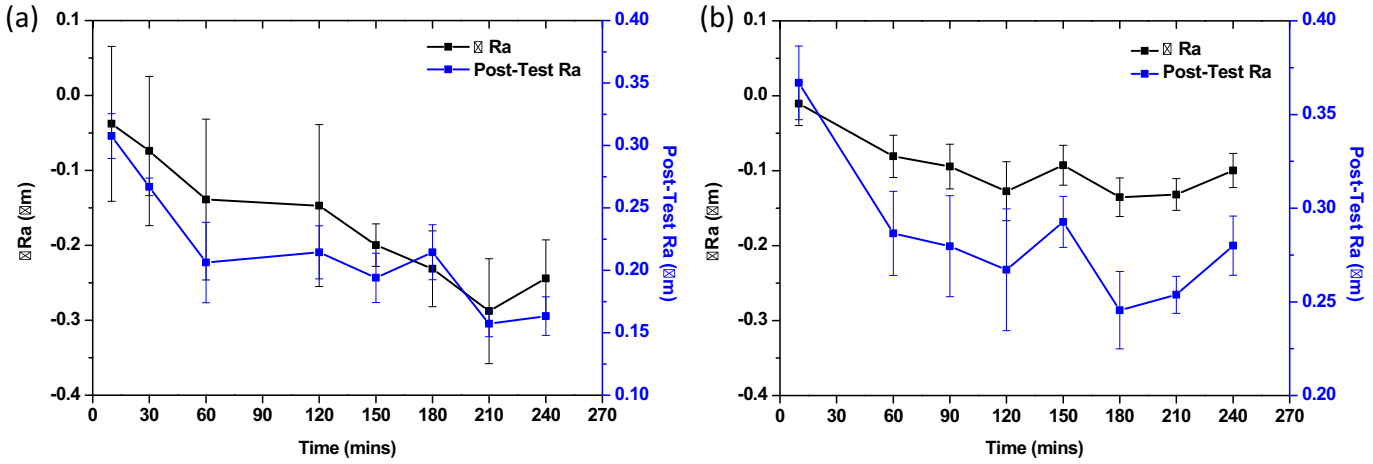

Fig. 6. ΔRa and post-test Ra of samples tested using (a) Pink Aggi and (b) Grey Ellipse media. Error bars represent the uncertainties of the measured data.

(Fig. 4a-b). High microscopic peaks are worn out first causing a flattening action, while the shallower areas which are shadowed by the surrounding high peaks retain the grainy appearance observed on the AD samples (Fig. 5a-b).

A higher presence of micro-abrasive marks is apparent as vibratory process time is increased. Compared to PA10, the surface of PA120 (Fig. 4c) shows a significantly bigger area of flattened peaks caused by the prolonged vibratory action. This results in the decrease of profile peak height values (Rp) with the increase of vibratory polishing time (Figs. 5c, SI 4). In contrast, the surface of GE120 shows the formation of larger and more pronounced wear tracks (Fig. 4d). The observed small and discontinuous tracks are associated with direct media impacts forming indentation marks (Fig. 5d). At the same process time, PA120 exhibit shallower wear tracks which can be attributed to the media geometry where the PA undergo more rolling with less scratching action compared to GE media. Prolonged vibratory polishing to 240 min does not show significant changes compared to samples polished for 120 min with similar polishing wear characteristics. The formation of deeper scratches on PA240, which are the characteristic of micro-ploughing, was more predominant on samples tested at this time duration (Fig. 4e). Similarly, the GE240 also exhibits pronounced wear tracks with varying lengths and widths (Fig. 4f). It is worth noting that the wear tracks formed with pink aggi media were also noticeably wider compared to grey ellipse due to the difference in media geometries where the tristar geometry of the pink aggi has more straight edges generating a bigger contact with the surface (Fig. 5e-f). Despite polishing for a total duration of 240 min, some areas still exhibit the as-deposited morphology, characterised by a grainy texture, suggesting that longer process times and a combination of different media used consecutively after each other might be required to achieve a completely smooth surface.

The change in Ra (ΔRa) of tested samples was calculated using Eq. (2) with results shown in Fig. 6a-b. Note that the negative values correspond to a drop in Ra. ΔRa of samples polished with PA is observed to decrease gradually in the first 60 min of polishing and then stabilise for up to 120 min. Further changes in Ra are observed to continue for the remaining test duration. An overall drop of ~0.25 μm was recorded, from the as-deposited to the vibratory polished condition. The change in Ra of samples tested with GE media was more abrupt than with pink media (Fig. 6a-b). GE10 samples exhibit ΔRa of 0.14 μm, while PA10 exhibit ΔRa of <0.05 μm. A more gradual ΔRa was observed throughout the whole process with an ultimate Ra of 0.18 μm reached after 240 min of polishing. In contrast, Ra of 0.16 μm was reached after 240 min of polishing with Pink Aggi. An overall ΔRa of 0.2 μm was recorded for the samples tested with Pink Aggi for the samples tested at the longest duration.

$$\Delta Ra = Ra_{(Polished)} - Ra_{(As-Deposited)} \quad (2)$$

4. Discussion

In general, our findings demonstrate the effectiveness of vibratory polishing in improving the surface finish of W/WC coatings. An ultimate Ra of 0.15–0.2 μm could be achieved with both PA and GE media over a duration of 4 h, which was a decrease in Ra of 0.2 μm from the as-deposited condition. As shown in Fig. 6a-b, Ra decreases with an increase in process time. The relatively small incremental drops in Ra can be attributed to the characteristic of W/WC coatings, which is highly

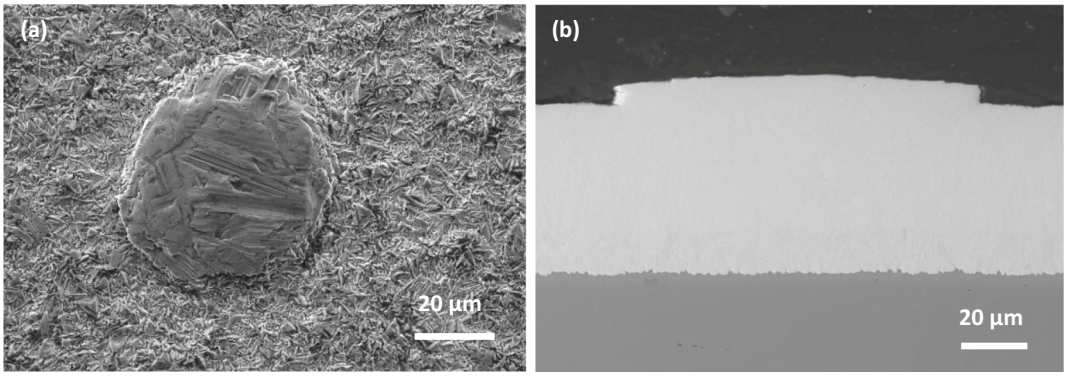

Fig. 7. (a) Surface and (b) cross-sectional view of polished surface nodule on PA240 sample.

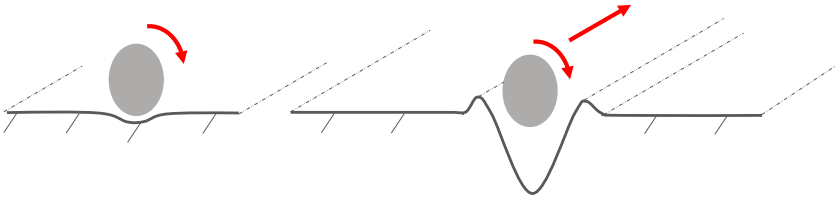

Fig. 8. Schematic diagrams showing: (a) rolling of media causing light scratching and (b) formation of micro-ploughing generated at longer vibratory exposure.

resistant to mechanical wear due to its high hardness. Compared to other techniques capable of processing parts with complex geometries such as electropolishing, vibratory polishing has proven to be a time-consuming process requiring significant process durations to achieve an Ra improvement of 0.2 μm from an initial Ra of 0.4 μm. Our previous work using electropolishing has shown that a mirror-like surface finish with an Ra of less than 0.05 μm is achievable on W/WC coatings with a hardness of 1300 HV within 5 min [10,11]. Therefore, from an efficiency and achievable level of surface finishing, vibratory polishing is a less preferred technique.

Nonetheless, vibratory polishing offers a benefit in terms of negligible change in coating thickness. As stated earlier, the thickness and weight of W/WC coatings remain constant even after being subjected to 240 min of vibratory polishing. In contrast, electropolishing results in a coating thickness loss of up to 18 μm to achieve a perfectly smooth planar surface [10,11]. These observations are in agreement with previous studies reported in literature [27], where the achievement of an undisturbed W surface through vibratory polishing required a significant amount of time (24 to 48 h) to match the same quality as that achieved with electropolishing. A major limitation of vibratory polishing was found to be its inability to remove nodules, which are isolated coating growths on the surface of the coating. After being subjected to vibratory polishing, the top area of the nodule is flattened but not completely removed (Fig. 7a-b), suggesting the inability of abrasive media to remove material from the top surface of the nodule as the surface area becomes bigger with process time. The morphology of the coating surrounding the nodule is retained in the as-deposited condition, suggesting that the surface nodule provides a shadowing affect preventing the abrasive media to reach the nodule's immediate surrounding area. Consequently, this results in the surface nodules being preferentially polished, while their immediate surrounding area remains unpolished.

Our SEM and AFM analysis suggest that abrasive wear is the predominant wear mechanism that operates in vibratory polishing [28,29]. Here, the contact of the fluidised abrasive media on the sample surface is characterised by rolling, scratching, and impact mechanisms [30]. For a short polishing duration, the abrasive effect is rather limited with only small patches of the surface being affected (Fig. 4a-b), suggesting that the different media geometry have a negligible polishing effect at short process durations. Note that most surface areas of the PA10 sample still appear to be unaffected, exhibiting the same morphology as that of the AD samples. Small craters observed on the surface of PA10 are the characteristic of free impacts, where the surface of the workpiece is simply struck by the abrasive media causing an isolated crater (Fig. 8a). This behaviour is in agreement with observations reported in previous studies following vibratory polishing of aluminum alloys [30–32]. Upon longer processing times, the formation of free impacts was observed to increase and the presence of abrasive wear became even more pronounced. The multi-directional scratch marks observed on the polished sample surfaces (Fig. 4c-f) suggest that the abrasive media undergo several flow fields during the process which reflects the stochastic nature of the process.

Apart from the formation of wear tracks due to scratching, micro-ploughing was found to be another predominant mechanism developing on the polished surfaces processed for longer times. Micro-ploughing was mostly observed on samples that have been polished for longer time duration with both PA and GE media. Micro-ploughing is a type of abrasive wear which occurs due to plastic deformation of the material without any material loss and is characterised by the formation of piled-up ridges to the sides of the wear track (Fig. 8b) [33]. Despite the occurrence of plastic deformation occurring on the surface of the coating, microhardness measurements taken at the surface of coated samples tested for 10 and 240 min did not show significant changes in comparison with the AD samples (Table *1*). The recorded Vickers microhardness ($HV_{0.05}$) measurements only show negligible average changes of $-2 < \Delta HV < 8$. Note that AD samples exhibit microhardness of 1330 ± 41 HV. As the change in hardness due to vibratory polishing is much smaller than the variation in hardness of the AD samples, this strongly suggests that work hardening is not a factor on W/WC samples processed through vibratory polishing. Despite the plastic deformation which was sustained throughout the entire duration of the polishing, the W/WC coating is free from cracks (Fig. 9).

Table 1
Change in microhardness results of polished samples (PA10, PA240, GE10 and GE 240) vs AD condition. HV_P is the average microhardness of the samples in the polished condition and HV_{AD} is the average microhardness of samples in the as-deposited coatings (1330 ± 41 HV). Here the microhardness results are shown as mean ± standard deviation values.

Sample	$\Delta HV = HV_P - HV_{AD}$
PA10	-2 ± 3
PA240	8 ± 7
GE10	-3 ± 8
GE240	4 ± 5

In many applications vibratory polishing is purposefully used for deburring and edge radiusing. However, when used as a surface finishing technique, it is essential that all the workpiece areas are uniformly polished without selective material removal around sharp edges, otherwise inconsistent coating thickness would result across the sample surface. Fig. 9a-b show an SEM surface view of a sample edge in the AD and PA240 which confirm that insignificant material loss with no functional material loss resulted after 240 min of vibratory polishing. This behaviour reflects not only the superior coating hardness but also the strong adhesion that exists between the coating and the substrate. Cross-sectional analysis of the coating around these edges confirms that other than a smoothening effect due to a reduction in surface roughness, vibratory polishing has a negligible effect on the change in coating thickness and to the functional properties of the coating.

The XRD patterns of vibratory polished W/WC coatings using Pink Aggi and Grey Ellipse for a duration of up to 210 min match those of the as-deposited samples (Fig. 10a). Here, all main detected peaks are attributed to crystalline W peaks with main crystallographic orientation of {110}, {200}, {211}, {220}, {310} and {321}. Unlike electropolishing that selectively removes certain electrochemically active grain orientation [11], vibratory polishing does not introduce any changes to the coatings' grain orientation. The absence of any WC peaks can be attributed to the nanocrystalline nature of WC dispersion in the W metal matrix that cannot be detected through XRD. Although WC nanocrystals

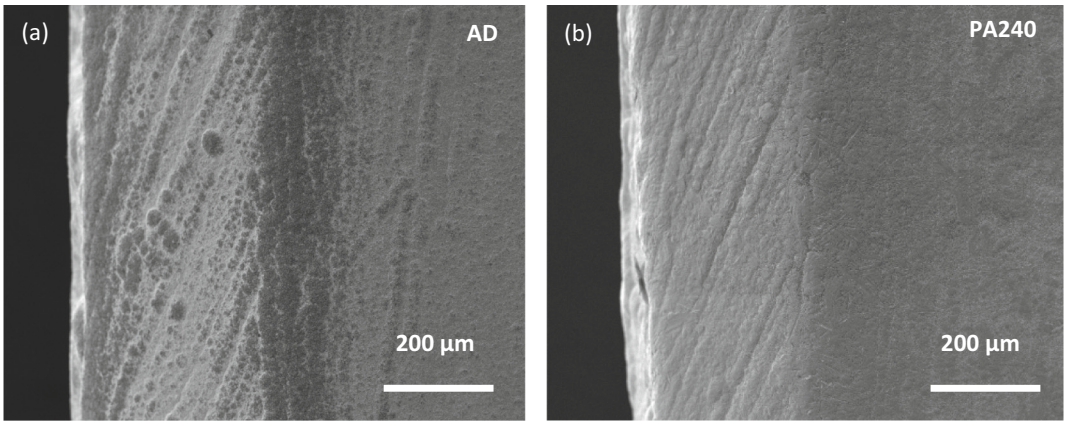

Fig. 9. Surface view of a sample edge in the (a) as-deposited and (b) vibratory polished condition for a duration of 240 min using Pink Aggi media.

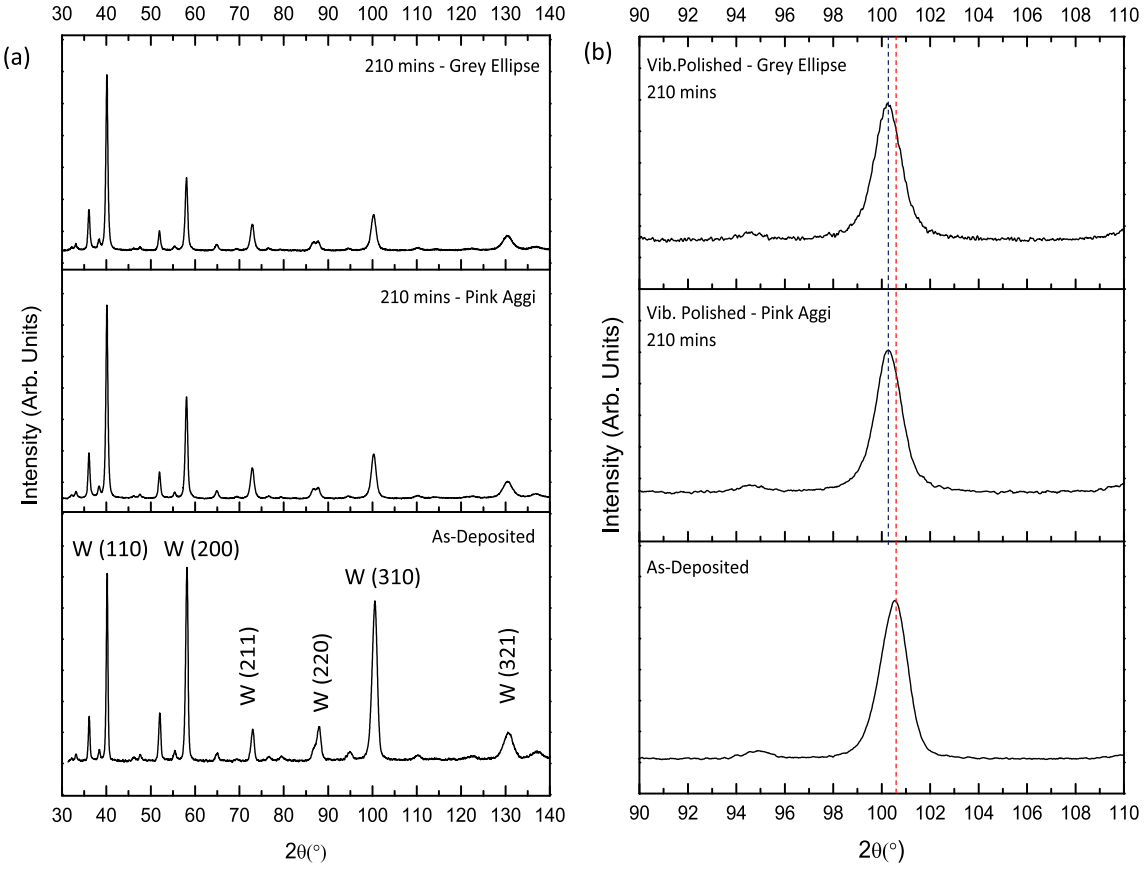

Fig. 10. XRD diffractogram of (a) as-deposited and vibratory polished W/WC coatings using Pink Aggi and Grey Ellipse media for a duration of 210 min and (b) a shift of the W (310) peak.

are not detected by XRD, our previous study using TEM has confirmed their presence within the W matrix [9]. A closer observation of the peaks acquired from the vibratory polished surfaces reveals a slight shift of the W {310} peak from the original 2θ position at 100.5° to a lower angle (Fig. 10b). Note that the shift in the W {310} peak is not accompanied by peak broadening, suggesting the homogeneity of the stresses across the coating. This implies that the impact of the media on the surface of the coating during the vibratory polishing lead to an increase in the compressive residual stress of the coating.

The shift of the W {310} peak motivates us to analyse the evolution of residual stresses of the W/WC coatings. The $\sin^2\psi$ method from X-ray diffraction patterns was employed to measure the magnitude and orientation of the residual stresses in the as-deposited and subsequently in the vibratory polished coatings. The angle (ψ) represents the angle of rotation of the sample about its surface normal, which is varied from -45^o to 45^o. The lattice spacing (d) is calculated using Bragg's law from the W {310} peak that are found between $96^o < 2\theta < 104^o$. Residual stress is then calculated from the coatings' Young's modulus (E) and Poisson's ratio (ν) along with the gradient of d vs $\sin^2\psi$ graph (m) (Eq. (1)). Here, E and ν are assumed to be constant with values of 400 GPa and 0.28 respectively. The d vs $\sin^2\psi$ graph of W/WC coatings shows negative gradient that implies the introduction of compressive residual

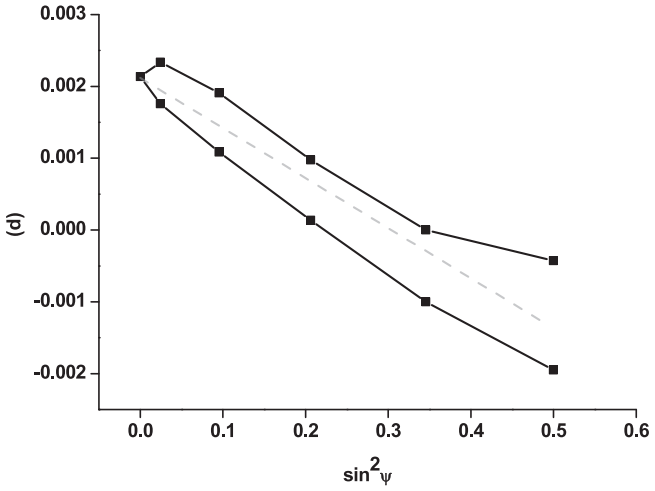

Fig. 11. d vs $sin^2\psi$ plot recorded for PA240 sample. Here d is the inter-planar spacing and ψ is the specimen orientation. The negative gradient signifies the compressive residual stress.

stresses by vibratory polishing (Fig. 11).

This analysis suggests that the magnitude of compressive residual stress in the coating increases with the vibratory polishing time, where the largest increases were recorded for samples tested for 120 min and over (Fig. 12a-b). This behaviour was observed on samples polished with both Pink Aggi and Grey Ellipse media, where an ultimate maximum compressive residual stress of −2890 MPa (Δ1058.3 MPa) and −2531.2 MPa (Δ631.2 MPa) was recorded for PA240 and GE240 respectively. Note that the negative value for residual stress corresponds to compressive stress. The increase in compressive residual stresses is in agreement with work reported in literature on titanium alloys subjected to vibratory peening [19]. Compressive residual stresses are usually beneficial in the surface layers of a material, as they lead to increased fatigue strength and stress corrosion cracking resistance that ultimately improve the service life of the material [32,34,35]. Despite this, excessive compressive residual stresses may also cause coating delamination within the coating and is typically manifested in the form of buckling [36]. Buckling due to excessive residual stresses is typical in thin films where pre-existent defects are present at the substrate–coating interface [37].

5. Conclusions

In this work we investigate the improvement in surface roughness of W/WC coatings through the use of two types of abrasive media with different geometries. This study suggests that vibratory polishing is a suitable surface finishing technique capable of processing parts with a deposited W/WC coating (hardness >1300 HV), resulting in no preferential loss of coating at the surface or sharp sample edges. Following 4 h of polishing, an average improvement in Ra of up to 0.2 μm and an ultimate surface finish of 0.15 μm was recorded for samples polished with both Pink Aggi and Grey Ellipse media with insignificant loss of material and change in coating thickness. Micro-abrasive wear and microploughing were found to be the predominant wear mechanisms, allowing an overall improvement in surface finish but with the formation of micro wear tracks. Insignificant changes in the microhardness of the coating were recorded for the samples tested at the longest durations. This implies that work hardening is not a factor on W/WC samples processed through vibratory polishing. For samples that have been polished for more than 30 min, the compressive residual stresses of the coating were observed to increase with time irrespective of which abrasive media was used. The increase in compressive residual stresses achieved with both media may be beneficial to the service life of the W/WC coatings due to the presumed increase to the coating's fatigue strength. In addition to negligible change in coating thickness, the ability to increase compressive residual stress is one of the key benefits of vibratory polishing. Nonetheless, from the perspective of efficiency and achievable level of surface finishing, vibratory polishing is a less preferred technique compared to electropolishing. The findings presented herein provide a baseline for further studies into surface finishing and residual stress engineering of hard coatings and difficult to process materials. This is highly relevant to numerous extreme engineering applications that require low surface roughness and stringent geometrical tolerance.

CRediT authorship contribution statement

Christian Micallef and Karl Walton conceived and planned the experiments in discussion with Adrianus Indrat Aria and Yuri Zhuk.

Karl Walton carried out the vibratory polishing tests at the University of Huddersfield.

Christian Micallef carried out the material characterization at Cranfield University and Hardide coatings.

Christian Micallef carried out the interpretation of results in discussion with Karl Walton, Adrianus Indrat Aria and Yuri Zhuk.

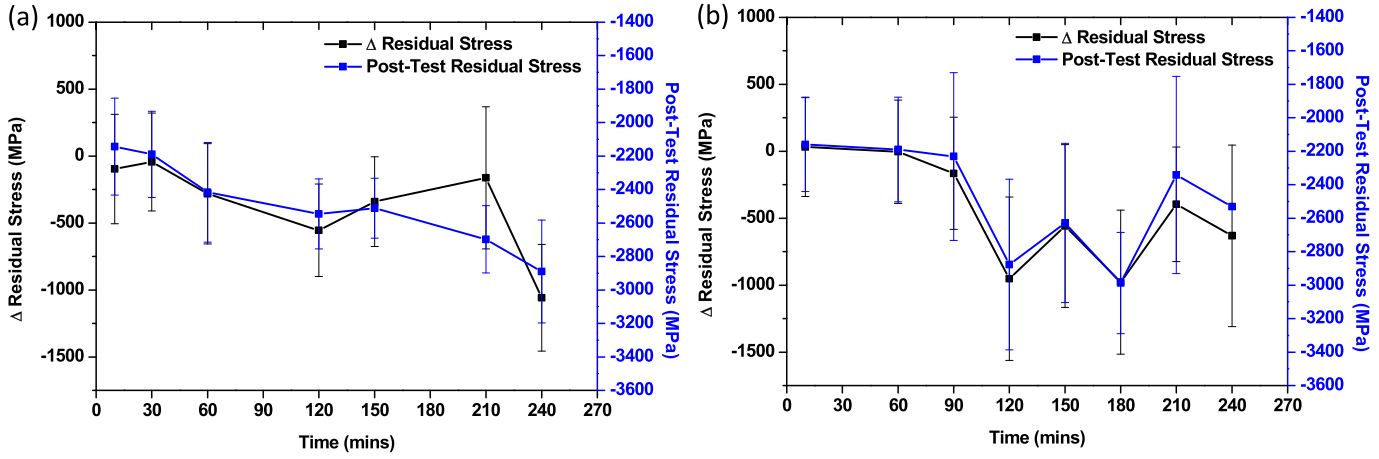

Fig. 12. Change in compressive residual stress and post-test residual stress of samples tested with (a) Pink Aggi and (b) Grey Ellipse media using the $sin^2\Psi$ method. Error bars represent the uncertainties of the measured data. Surface stresses for W/WC coating in the as-deposited and vibratory polished conditions at different time durations using the $sin^2\Psi$ method. The connecting solid lines are only guides for the eye. Negative value for residual stress corresponds to compressive stress.

The first draft of the manuscript was written by Christian Micallef with support from Adrianus Indrat Aria, Karl Walton and Yuri Zhuk.

Adrianus Indrat Aria, Yuri Zhuk and Karl Walton provided the supervision throughout the course of conducting this research work and preparation of the presented manuscript.

All authors reviewed the results and approved the final version of the manuscript.

Declaration of competing interest

We declare that the submitted article has not been submitted in any other journal and is not under consideration for publication elsewhere. We also declare that two of the authors, Christian Micallef and Yuri Zhuk, are both directly employed by Hardide Coatings plc.

Appendix A. Supplementary data

Supplementary data to this article can be found online at https://doi.org/10.1016/j.surfcoat.2022.128447. Data underlying this study can be accessed through CORD at https://doi.org/10.17862/cranfield.rd.19597210.v1

References

[1] G. Schuhler, A. Jourani, S. Bouvier, J.M. Perrochat, Efficacy of coatings and thermochemical treatments to improve wear resistance of axial piston pumps, Tribol. Int. 126 (2018) 376–385, https://doi.org/10.1016/j.triboint.2018.05.007.

[2] S. Paul, Special issue: “Coatings for harsh environments”, Coatings 10 (2020) 10–13, https://doi.org/10.3390/coatings10040407.

[3] D. Ma, T.J. Harvey, Y.N. Zhuk, R.G. Wellman, R.J.K. Wood, Cavitation erosion performance of CVD W/WC coatings, Wear 452–453 (2020), 203276, https://doi.org/10.1016/j.wear.2020.203276.

[4] Y.N. Zhuk, Nano-structured CVD Tungsten Carbide coating protects against wear and corrosion, in: Proceedings of the Corrosion 2010, 2010, pp. 1–15. San Antonio, Texas.

[5] K. Zheng, H. Hu, F. Chen, Y. Zheng, Failure analysis of the blackwater regulating valve in the coal chemical industry, Eng. Fail. Anal. 125 (2021), 105442, https://doi.org/10.1016/j.engfailanal.2021.105442.

[6] R.A. Mahdavinejad, A. Mahdavinejad, ED machining of WC-Co, J. Mater. Process. Technol. 162–163 (2005) 637–643, https://doi.org/10.1016/j.jmatprotec.2005.02.211.

[7] J. Solis, H. Zhao, C. Wang, J.A. Verduzco, A.S. Bueno, A. Neville, Tribological performance of an H-DLC coating prepared by PECVD, Appl. Surf. Sci. 383 (2016) 222–232, https://doi.org/10.1016/j.apsusc.2016.04.184.

[8] D. Jianxin, Z. Hui, W. Ze, L. Yunsong, Z. Jun, Friction and wear behaviors of WC/Co cemented carbide tool materials with different WC grain sizes at temperatures up to 600 °C, Int. J. Refract. Met. Hard Mater. 31 (2012) 196–204, https://doi.org/10.1016/j.ijrmhm.2011.11.003.

[9] C. Micallef, Y.N. Zhuk, R.J.K. Wood, Galling resistance of nanostructured CVD tungsten/tungsten carbide coatings, Surf. Topogr. Metrol. Prop. 7 (2019), https://doi.org/10.1088/2051-672X/ab1535.

[10] C. Micallef, Y. Zhuk, A.I. Aria, Recent progress in precision machining and surface finishing of tungsten carbide hard composite coatings, Coatings 10 (2020) 1–36, https://doi.org/10.3390/coatings10080731.

[11] C. Micallef, C.-W. Chiu, Y. Zhuk, A.I. Aria, Rapid surface finishing of chemical vapour deposited tungsten carbide hard coatings by electropolishing, Surf. Coat. Technol. 428 (2021), 127900, https://doi.org/10.1016/j.surfcoat.2021.127900.

[12] Y.N. Zhuk, HardideTM: advanced nano-structured CVD coating, Int. J. Microstruct. Mater. Prop. 2 (2007) 90–98, https://doi.org/10.1504/IJMMP.2007.012942.

[13] Substances restricted under REACH, Available online: https://echa.europa.eu/substances-restricted-under-reach (accessed on Aug 26, 2021).

[14] C. Kainz, N. Schalk, M. Tkadletz, C. Mitterer, C. Czettl, Microstructure and mechanical properties of CVD TiN/TiBN multilayer coatings, Surf. Coat. Technol. 370 (2019) 311–319, https://doi.org/10.1016/j.surfcoat.2019.04.086.

[15] K. Nakanishi, A.I. Aria, M.F. Berwind, R.S. Weatherup, C. Eberl, S. Hofmann, N. A. Fleck, Acta materialia compressive behavior and failure mechanisms of freestanding and composite 3D graphitic foams, Acta Mater. 159 (2018) 187–196, https://doi.org/10.1016/j.actamat.2018.08.012.

[16] T. Cebo, A.I. Aria, J.A. Dolan, R.S. Weatherup, K. Nakanishi, P.R. Kidambi, G. Divitini, C. Ducati, U. Steiner, S. Hofmann, et al., Chemical vapour deposition of freestanding sub-60 nm graphene gyroids chemical vapour deposition of freestanding sub-60 nm graphene gyroids, Appl. Phys. Lett. 111 (2017).

[17] D. Bańkowski, S. Spadło, Influence of the smoothing conditions in vibro-abrasive finishing and deburring process for geometric structure of the surface machine parts made of aluminum alloys en AW-2017A, in: Met. 2015 - 24th Int. Conf. Metall. Mater. Conf. Proc, 2015, pp. 1062–1068. San Antonio, Texas.

[18] M.D. Sangid, J.A. Stori, P.M. Ferriera, Process characterization of vibrostrengthening and application to fatigue enhancement of aluminum aerospace components-part II: process visualization and modeling, Int. J. Adv. Manuf. Technol. 53 (2011) 561–575, https://doi.org/10.1007/s00170-010-2858-1.

[19] L. Canals, J. Badreddine, B. McGillivray, H.Y. Miao, M. Levesque, Effect of vibratory peening on the sub-surface layer of aerospace materials Ti-6Al-4V and E-16NiCrMo13, J. Mater. Process. Technol. 264 (2019) 91–106, https://doi.org/10.1016/j.jmatprotec.2018.08.023.

[20] P.P. Kumar, S. Sathyan, Simulation of 1D abrasive vibratory finishing process, Adv. Mater. Res. 565 (2012) 290–295, https://doi.org/10.4028/www.scientific.net/AMR.565.290.

[21] S. Wang, R.S. Timsit, J.K.S., Experimental investigation of fixtured vibratory finishing of aluminium, Lect. Notes Eng. Comput. Sci. 2224 (2016) 714–718.

[22] A.S. Metel, S.N. Grigoriev, T.V. Tarasova, A.A. Filatova, S.K. Sundukov, M. A. Volosova, A.A. Okunkova, Y.A. Melnik, P.A. Podrabinnik, Influence of postprocessing on wear resistance of aerospace steel parts produced by laser powder bed fusion, MDPI Technol. 8 (2020), https://doi.org/10.3390/technologies8040073.

[23] T. Bergs, U. Müller, S. Barth, M. Ohlert, Experimental analysis on vibratory finishing of cemented carbides, Manuf. Lett. 28 (2021) 21–24, https://doi.org/10.1016/j.mfglet.2021.02.004.

[24] C. Micallef, Y.N. Zhuk, R.J.K. Wood, Galling resistance of nanostructured CVD tungsten/tungsten carbide coatings, Surf. Topogr. Metrol. Prop. 7 (2019) 25004, https://doi.org/10.1088/2051-672X/ab1535.

[25] M.E. Fitzpatrick, A.T. Fry, NPL Good Practice Guide No. 52: Determination of Residual Stresses by X-ray Determination of Residual Stresses by X-ray Diffraction - Issue 2, 2005.

[26] S. Shoja, N. Mortazavi, E. Lindahl, S. Norgren, O. Bäcke, M. Halvarsson, Microstructure investigation of textured CVD alumina coatings, Int. J. Refract. Met. Hard Mater. 87 (2020), 105125, https://doi.org/10.1016/j.ijrmhm.2019.105125.

[27] S. Pathak, S.R. Kalidindi, Spherical nanoindentation stress-strain curves, Mater. Sci. Eng. R Rep. 91 (2015) 1–36, https://doi.org/10.1016/j.mser.2015.02.001.

[28] A. Sofronas, S. Taraman, Model development and optimization of vibratory finishing process, Int. J. Prod. Res. 17 (1979) 23–31, https://doi.org/10.1080/00207547908919592.

[29] J. Domblesky, R. Evans, V. Cariapa, Material removal model for vibratory finishing, Int. J. Prod. Res. 42 (2004) 1029–1041, https://doi.org/10.1080/00207540310001619641.

[30] A. Yabuki, M.R. Baghbanan, J.K. Spelt, Contact forces and mechanisms in a vibratory finisher, Wear 252 (2002) 635–643, https://doi.org/10.1016/S0043-1648(02)00016-9.

[31] M.R. Baghbanan, A. Yabuki, R.S. Timsit, J.K. Spelt, Tribological behavior of aluminum alloys in a vibratory finishing process, Wear 255 (2003) 1369–1379, https://doi.org/10.1016/S0043-1648(03)00124-8.

[32] R. Mediratta, K. Ahluwalia, S.H. Yeo, State-of-the-art on vibratory finishing in the aviation industry: an industrial and academic perspective, Int. J. Adv. Manuf. Technol. 85 (2016) 415–429, https://doi.org/10.1007/s00170-015-7942-0.

[33] T. Mishra, G.C. Ganzenmüller, M. de Rooij, M. Shisode, J. Hazrati, D.J. Schipper, Modelling of ploughing in a single-asperity sliding contact using material point method, Wear 418–419 (2019) 180–190, https://doi.org/10.1016/j.wear.2018.11.020.

[34] F.A. Kandil, J.D. Lord, A.T. Fry, P. Grant, A Review of Residual Stress Measurement Methods - A Guide to Technique Selection, 2001. Teddington, Middlesex UK.

[35] D. Karlsson, Residual Stress in CVD Coatings Evaluation of XRD and TEM Methods for Micro and Macrostress Determination Residual Stress in CVD Coatings, Upsalla University, 2015.

[36] S. Eroglu, B. Gallois, Residual stresses in chemically vapor deposited coatings in the Ti-C-N system, J. Phys. IV 3 (1993) 155–162, https://doi.org/10.1051/jp4:1993319.

[37] A.R. Shugurov, A.V. Panin, Mechanisms of stress generation and relaxation in thin films and coatings, AIP Conf. Proc. 1623 (2014) 575–578, https://doi.org/10.1063/1.4899010.